Title
ANGLE-RESOLVED XPS ANALYSIS OF OXIDIZED POLYCRYSTALLINE SiC SURFACES

Authors
Rahaman, M.N.
Jonghe, L.C. De

Publication Date
1986-04-01

Lawrence Berkeley Laboratory
UNIVERSITY OF CALIFORNIA

Materials & Molecular Research Division

Submitted to Journal of the American Ceramic Society

ANGLE-RESOLVED XPS ANALYSIS OF OXIDIZED POLYCRYSTALLINE SiC SURFACES

M.N. Rahaman and L.C. De Jonghe

April 1986

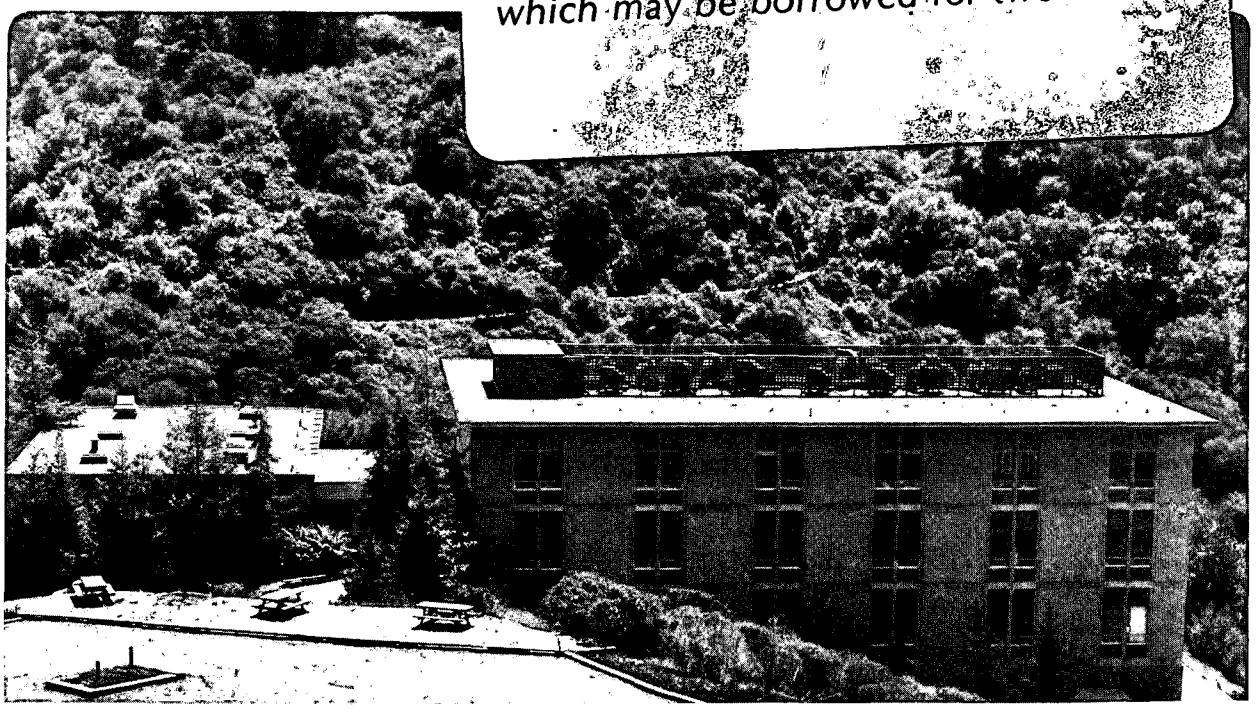

Prepared for the U.S. Department of Energy under Contract DE-AC03-76SF00098

DISCLAIMER

ANGLE-RESOLVED XPS ANALYSIS OF OXIDIZED POLYCRYSTALLINE SiC SURFACES

M. N. Rahaman*, and L. C. De Jonghe*
Materials and Molecular Research Division
Lawrence Berkeley Laboratory
and
University of California
Berkeley, California 94720

ABSTRACT

The nature of surface oxide and of adsorbed hydrocarbons (or free carbon) on dense, polycrystalline silicon carbide has been studied using angle-resolved x-ray photoelectron spectroscopy (XPS). The oxide appears to be very close to the composition of SiO_2 and no evidence was found for a change in the composition with depth from the surface. The thicknesses of the silica and the hydrocarbon layers were also estimated from expressions for the x-ray photoelectron intensity. The results are consistent with a model consisting of bulk silicon carbide covered by a silica layer $\sim$1.2 nm thick, which in turn is covered by $\sim$1-2 monolayers of adsorbed hydrocarbons.

Supported by the Division of Materials Sciences, Office of Basic Energy Sciences, U. S. Department of Energy, under Contract No. DE-AC03-76SF00098

*Member, the American Ceramic Society.

I. INTRODUCTION

Silicon carbide and silicon nitride materials are currently used in a number of industrial applications and are also considered for high temperature load bearing applications, such as heat engines. These materials are made from powders by processes that involve consolidation and sintering (with or without applied pressure). The surfaces of the powders (and the final, dense article) are invariably covered by a native oxide (or oxygen-rich) layer having a thickness of a few nanometers. It is widely recognized that the oxide layer on the powders has a profound effect on their processing behavior and on the properties of the final article.

In previous work[1], the surfaces of commercial silicon nitride and silicon carbide powders have been characterized using high-voltage and high-resolution transmission electron microscopy (TEM), x-ray photoelectron spectroscopy (XPS), and secondary ion mass spectrometry (SIMS). These powders were made by reactions at high temperatures, typically above $\sim$1300^{o}C. TEM has shown that the oxide layer is amorphous and is $\sim$3-5 nm thick. The XPS results have suggested that the oxide layer on the silicon nitride powders has, in part, the comoposition of a silicon oxynitride, rather than silica, but the oxide layer on the silicon carbide powders has a composition similar to silica. These compositions are really an average over the depth sampled by the XPS analysis, typically $\sim$5 nm.

For powders, the surface sensitivity of XPS cannot be varied by angle-resolved studies because of the particulate microgeometry of the sample. Thus, any changes in elemental concentration with distance from the surface would have to be inferred from angle-resolved XPS studies on flat, solid samples. Raider et al.[2] have studied the controlled oxidation of clean silicon nitride films using XPS. Their results have shown that the oxidized layer formed is a 'graded' oxynitride, with the elemental concentration of oxygen decreasing steadily with distance from the surface.

This study deals with the use of the angle-resolved XPS technique to study the nature of the oxide layer on dense, polycrystalline silicon carbide. The main aims are, first, to investigate any change in elemental concentration with depth from the surface, and second, to estimate the thickness of the oxide layer.

II. EXPERIMENTAL

The sample used for XPS, 5 mm square and of nearly uniform thickness of 1 mm, was cut from a hot-pressed, solid disc of silicon carbide.* One surface was then ground and polished using diamond paste and a non-aqueous lubricant to remove both the existing oxide layer and any surface roughness. The surfaces of the sample were cleaned by washing in methanol and acetone and dried for 24 hours in a vacuum

*Norton Company, Worcester, Mass.

furnace at 60 °C. The sample was then reoxidized at room temperature for ~1 week. The oxide layer on the sample used for XPS is therefore representative of a clean polycrystalline surface subject to room temperature oxidation.

X-ray photoelectron spectroscopy (XPS) was performed in a Physical Electronics 548 Auger/ESCA system. The spectrometer used a MgK_{α} (1253.6 eV) x-ray source and a double-pass cylindrical mirror analyzer (CMA). The system is ion pumped with a base pressure of $4x10^{-8}$ Pa. The sample was introduced into the analysis chamber by a rapid probe. It was first analyzed for the spectra of Si(2*p*), C(1*s*) and O(1*s*), with the data collected over all take-off angles. Spectra of these elements were then recorded at specific take-off angles of 0, 25, 40, 55 and 70 degrees relative to the normal of the sample. The data collection and analysis system used for XPS has been described in detail elsewhere.[3]

III. THEORETICAL

(a) Equations for the Photoelectron Intensity.

A calculation of the surface composition from XPS requires a set of equations for the x-ray photoelectron intensities that reflect the surface layering of the sample. The set of equations used in this study follows the treatment of Dreiling[4] for a general system of several homogeneous layers. Generally, the equations for the photoelectron intensities are derived assuming an exponential attenuation of electron intensity during passage through the solid.

For an element i, the photoelectron intensity from an incremental layer at depth z into the surface can then be expressed as

$$dI_i = I_{oi} \exp(-z/g\lambda_i)dz \tag{1}$$

where I_{oi} is the number of photoelectrons generated per unit volume, λ_i is the mean free path of the electrons of kinetic energy E_i, and g is an instrumental factor that takes into account the angle of escape of the electron with respect to the surface normal. The quantity I_{oi} is given by

$$I_{oi} = K_o \sigma_i x_i \tag{2}$$

where K_o is a constant instrumental factor, x_i is the atomic volume concentration and σ_i is the photoelectron cross section. The XPS system used in this study utilizes a CMA operating in the retarding grid mode, and for this, the transmission of electron varies[5] as $1/E_i$. The detected incremental intensity can then be written as

$$dI_i = (K\sigma_i x_i/E_i) \exp(-z/g\lambda_i)dz \tag{3}$$

where K is an instrumental constant. In general, the total intensity, I_i^B, at an angle θ to the surface normal, for a bulk substrate covered by a surface layer of thickness z and having x_i^B, atoms of the element i per unit volume is given by

$$I_i^B = (K\sigma_i x_i^B g\lambda_i/E_i) \exp(-z/g\lambda_i \cos\theta) \tag{4}$$

The total intensity, I_k^S, from the surface layer of element k is correspondingly

$$I_k^S = (K\sigma_k x_k^S g\lambda_k/E_k)[1 - \exp(-z/g\lambda_k \cos\theta)] \quad (5)$$

(b) Model for Silicon Carbide

Earlier work[1] on silicon carbide powders showed that the particles are covered by an amorphous oxide layer, presumably silica, Fig. 1, and that a small amount of hydrocarbons (or free carbon) is also present on the surface. Thus, a useful starting model for the surface of silicon carbide is shown in Fig. 2. It consists of a bulk substrate silicon carbide containing atomic densities x_{Si}^B and x_C^B of Si and C respectively. The bulk is then immediately covered by an (intermediate) silica layer of thickness y nm, containing atomic densities x_{Si}^I and x_O^I of Si and O respectively. Finally, the surface is covered with a hydrocarbon layer, z nm thick, containing atomic densities x_C^S and x_H^S of C and H respectively.

The x-ray photoelectron intensity equations for this model are summarized in Table I. The electron mean free path, λ_i, for an element i in units of 'monolayers' is estimated using an empirical relation given by Chang[6], i.e.

$$\lambda_i = 0.2E_i^{1/2} \quad (6)$$

where E_i is the kinetic energy of the electron. The definition of a monolayer is taken as the cube edge length of the average volume per atom in the surface layers or in the bulk. The instrument geometrical

factor, g, is taken to be equal to 0.74, the value calculated by Seah[7] for a cylindrical mirror analyzer.

Table I: X-ray photoelectron intensity equations for the silicon carbide surface model shown in Fig. 1.

Surface Layer	$I_C^S = K_C^S x_C^S [1 - \exp(-z/g\lambda_C^S \cos\theta)]$	(a)
	$I_H^S = K_H^S x_C^S [1 - \exp(-z/g\lambda_H^S \cos\theta)]$	(b)
Intermediate Layer	$I_{Si}^I = K_{Si}^I x_{Si}^I [1 - \exp(-y/g\lambda_{Si}^I \cos\theta)] \exp(-z/g\lambda_i^I \cos\theta)$	(c)
	$I_0^I = K_0^I x_0^I [1 - \exp(-y/g\lambda_0^I \cos\theta)] \exp(-y/g\lambda_0^I \cos\theta)$	(d)
Bulk	$I_{Si}^B = K_{Si}^B x_{Si}^B \exp[-(y+z)/g\lambda_{Si}^B \cos\theta]$	(e)
	$I_C^B = K_C^B x_C^B \exp[-(y+z)/g\lambda_C^B \cos\theta]$	(f)

IV. RESULTS AND DISCUSSION

(a) Angle-Resolved X-ray Photoelectron Spectra

Fig. 3 shows the Si (2*p*) line spectrum for the silicon carbide sample at take-off angles of (a) 0^o, (b) 40^o, and (c) 70^o, relative to the surface normal. Each spectrum consists of two peaks. The peak positions have to be corrected for static charging of the sample. The C (1_s) peak arising from hydrocarbons or free carbon was used as a reference and its position[8] was taken as 284.6 eV. The peak at lower

binding energy (~100.5 - 100.7 eV) decreases in intensity with increasing take-off angles and is due to Si in the bulk SiC. the peak at higher binding energy (~103.1 eV) increases with increasing take-off angle and is due to Si in a surface layer of SiO_2. Previous work[2,8] involving standards has shown that SiO_2 has Si(2p) at ~103 - 103.5 eV.

Table II shows the Si(2p) peak positions in SiC and SiO_2 for the three take-off angles, and the difference in these two peak positions, ΔSi(2p). The error in these peak positions is estimated to be $\pm$ 0.1 eV, due mainly to the corrections for static charging and to the curve fitting routine. Within the limits of experimental error, the peak positions are independent of the take-off angle. Thus, for this sample of SiC, there appears to be almost no change in chemical composition within the SiO_2 layer. This is also supported by the results for the O(1s) line spectrum. This spectrum consists of a single peak at 532.5 eV and the peak position is very close to the value of ~532.7 eV obtained by Raider et al[2] for the O(1s) peak in SiO_2. In addition, there is no change in the O(1s) peak half-width at the different take-off angles.

Table II: Peak positions of Si(2p) in SiC and SiO_2, as well as the difference in these two peak positions, at different take-off angles.

Take-off Angle (Degrees)	Si (2p) (eV) SiC	SiO_2	ΔSi(2p) (eV)
0	100.5	103.0	2.5
40	100.6	103.1	2.5
70	100.7	103.0	2.3

Further support for no compositional change in the SiO_2 layer is obtained from a plot of the O(1s) to Si(2p) (at ~103.1 eV) line intensity ratio as a function of the take-off angle, θ, shown in Fig. 4. This ratio would be expected to increase with increasing θ if there were a decrease in oxygen concentration with depth from the surface of the silica layer. The results show that the O(1s) / Si(2p) line intensity ratio is almost independent of θ.

Fig. 5 shows the C(1s) line spectrum at take-off angles of (a) 0^0, (b) 40^0, and (c) 70^0 (relative to the sample surface normal). At any angle, the best fit to the data is obtained using three peaks, at ~282.7, 284.6 and ~286.0 eV, after correcting for static charging. The peak at ~282.7 eV is due to carbon in the bulk SiC; its intensity decreases with increasing θ. The peak at 284.6 eV is due to hydrocarbons in the surface layer. From its variation with θ, it appears that the minor peak at ~286.0 eV is due to a surface species

but its chemical environment is difficult to assign because of its low intensity and the possibility of differential charging.

(b) Estimation of Surface Layer Thickness

In estimating the thicknesses y and z of the intermediate (SiO_2) layer and the surface (hydrocarbon) layer, respectively, from equations (a) - (f) in Table I, it should be pointed out that a plot of ln (I_i) versus cos θ cannot be used, since for the spectrometer used, K_i contains angle-dependent terms.

For the present study, y can be conveniently obtained by a ratio method, using the Si(2p) intensities from the oxide layer I^I_{Si} and from the bulk, I^B_{Si}. In addition from equation 6, it is found that $\lambda^I_{Si} \sim \lambda^B_{Si} \cong 1.8$ nm. Then at a fixed take-off angle θ, $K^I_{Si} \sim K_{Si}$. Using these relations,

$$I^B_{Si}/I^I_{Si} = x^B_{Si}[e^{-\alpha}/(1 - e^{-\alpha})]/x^I_{Si} \qquad (7)$$

where $\alpha = y/(g\lambda_{Si} \cos \theta)$

The atomic density, x_i, of element i in a compound M may be calculated from the density and molecular weight of M.

Similarly, for evaluating z, equations (a) and (f) in Table I may be used. Assuming the hydrocarbon layer has a composition approximating $(C_2H_4)_n$, then $\lambda_C^S \sim \lambda_C^B \cong 1.3$ nm, and $K_C^S \sim K_C^B$. Thus:

$$I_C^B/I_C^S = x_C^B[e^{-(\beta+\gamma)}/(1 - e^{-\beta})]/x_C^S \qquad (8)$$

where $\beta = z/(g\lambda_C \cos\theta)$ and $\gamma = y/(g\lambda_C \cos\theta)$. The surface layer thicknesses, y and z, can now be evaluated at various values of θ, first by finding y from equation (7) and then by substituting in equation (8).

Figure 6 shows the results for y and z versus the take-off angle θ. It is seen that for θ between 25^0 and 55^0, y is nearly constant and is equal to ~1.2 nm. z is also relatively constant within this range of θ and is equal to ~0.3 nm. The deviations in the layer thicknesses determined by angle-resolved XPS have been explained[9-11] in terms of the spectrometer count-rate statistics at low θ and in terms of surface roughness of the sample for θ values greater than $\sim 60^0$. A contribution to this effect at large may also come from elastically scattered photoelectrons.[12]

It should be pointed out that both y and z are proportional to the electron mean free path, λ_i, calculated from Eqn. (6). There remains considerable uncertainty in the relationship between λ_i and the electron kinetic energy E_i. Equation (6) should thus be replaced by a more reliable one in the future.

V. CONCLUSIONS

The technique of angle-resolved x-ray photoelectron spectroscopy (XPS) has been used to study the composition and thickness of the oxide layer and contaminants on polycrystalline silicon carbide. For this sample, ground and polished, then oxidized in air at room temperature for ~1 week, the oxide layer has a composition very close to SiO_2. No evidence was found for a change in oxygen concentration with depth from the surface of this layer. The thickness of the SiO_2 layer was estimated to be ~1.2 nm. The SiO_2 layer is in turn covered by a hydrocarbon (or free carbon) layer estimated to be ~0.3 nm thick.

Acknowledgments: The authors wish to thank B. C. Beard and P. N. Ross, Jr., for helpful discussions. In addition, B. C. Beard provided technical help in using the XPS equipment.

REFERENCES

1. M. N. Rahaman, Y. Boiteux and L. C. De Jonghe "Surface Characterization of Silicon Nitride and Silicon Carbide Powders" Amer. Ceram. Soc. Bull., to be published.

2. S. I. Raider, R. Flitsch, J. A. Aboaf, and W. A. Plisken "Surface Oxidation of Silicon Nitride Films" J. Electrochem. Soc. 123 4 560-65 (1976).

3. B. C. Beard, D. Dahlgren, and P. N. Ross, Jr., "Microcomputer-Multichannel Analyzer Data System for Fore-ground - Background Data Collection and Analysis" J. Vac. Sci. Tech. (A) 3 5 2041-43 (1985).

4. M. J. Dreiling "Quantitative Surface Measurements of Metal Oxide Powders" Surface Sci., 71 231-46 (1978).

5. P. W. Palmberg "A Combined ESCA and Auger Spectrometer" J. Vac. Sci. Tech. 12 1 379-84 (1975).

6. C. C. Chang "General Formalism for Quantitative Auger Analysis Surface Sci., 48 9-21 (1975).

7. M. P. Seah "Quantitative Auger Electron Spectroscopy and Electron Ranges" Surface Sci., 32 703-28 (1972).

8. C. D. Wagner, W. M. Riggs, L. E. Davis, J. F. Moulder and G. E. Muilenberg (ed.), "Handbook of X-ray Photoelectron Spectroscopy" Perkin-Elmer Corp., MN 55344 (1978).

9. M. F. Ebel "Determination of Reduced Thicknesses of Means of the Variable Take-Off Angles Technique" J. Electron. Spectrosc. Relat. Phenon., 22 333-46 (1981).

10. M. F. Ebel, H. Ebel, and K. Hirokawa "Quantitative Analysis by X-ray Photoelectron Spectroscopy Without Reference Samples" Spectrochim. Acta 37B 6 461-71 (1982)

11. M. F. Ebel, G. Zuba, H. Ebel, J. Wernisch, and A. Jablonski "Film Thicknesses Determined by X-ray Photoelectron Spectroscopy" Spectrochim. Acta 39B 5 637-47 (1984)

12. O. A. Baschenko and V. I. Nefedov "Relative Intensities in X-ray Photoelectron Spectra, VII: The Effect of Elastic Scattering in a Solid on the Angular Distribution of Photoelectrons Escaping from Samples Covered with Thin Films of Various Thicknesses" J. Electron Spectrosc. Relat. Phenom. 21 153-69 (1980)

LIST OF FIGURES

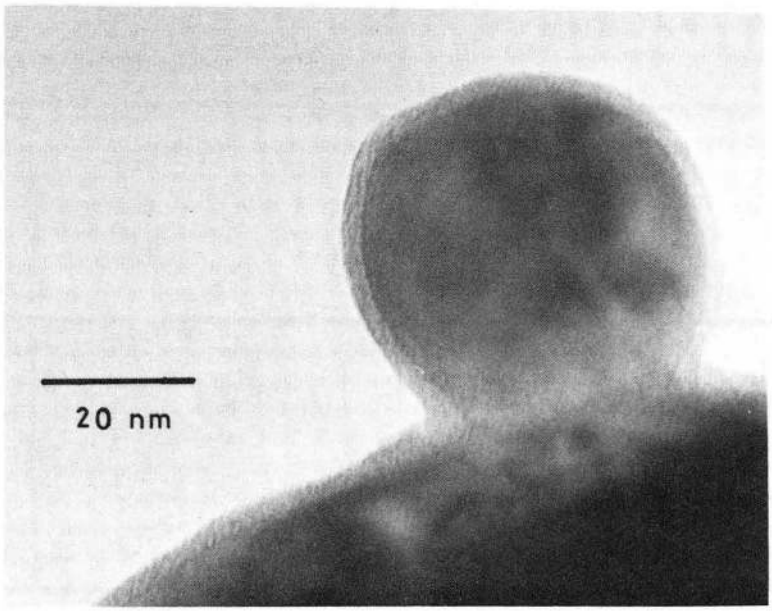

XBB 864-3436

Fig. 1

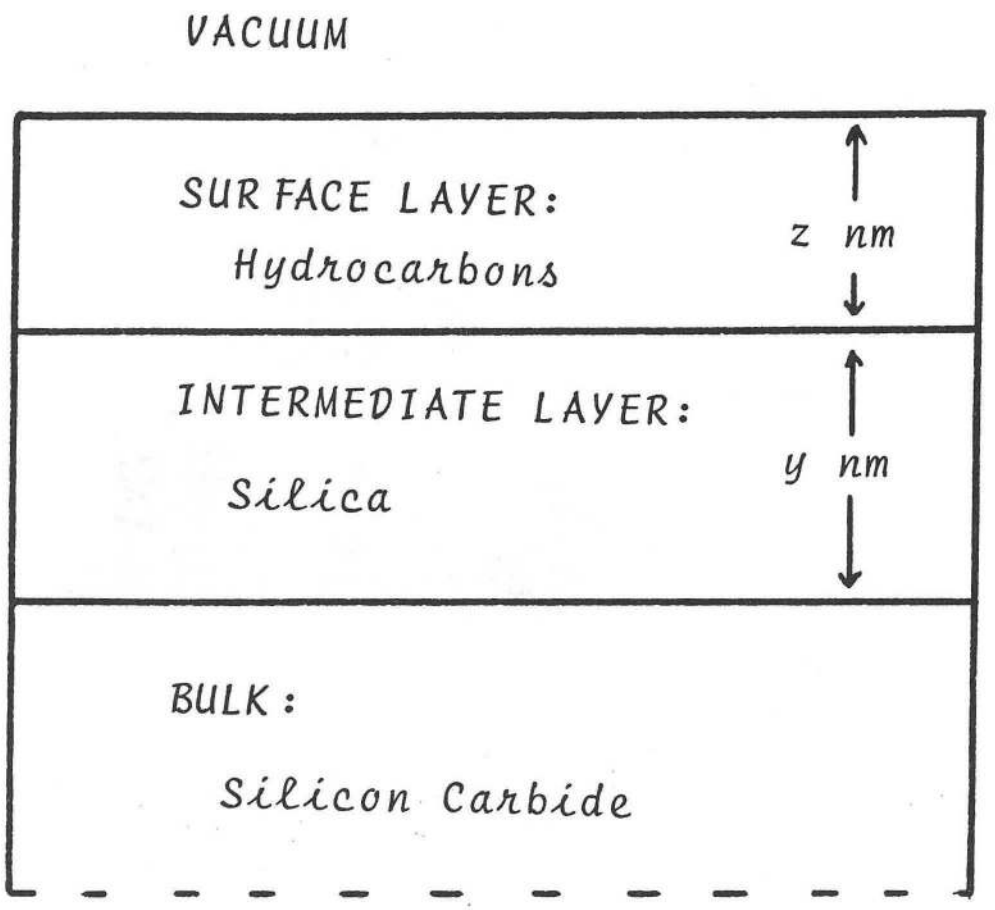

XBL 864-1662

Fig. 2

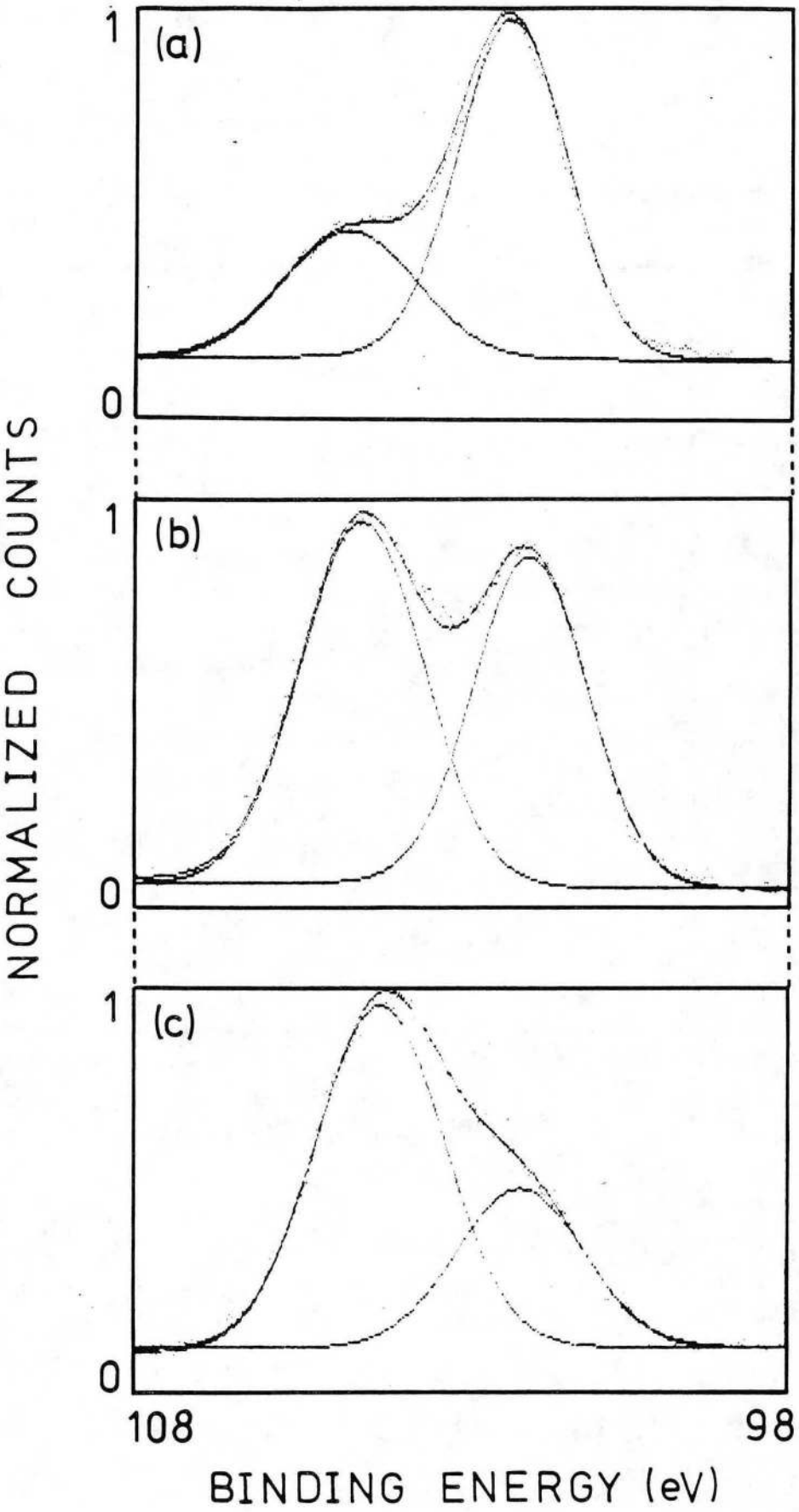

Fig. 3

XBL 865-1725

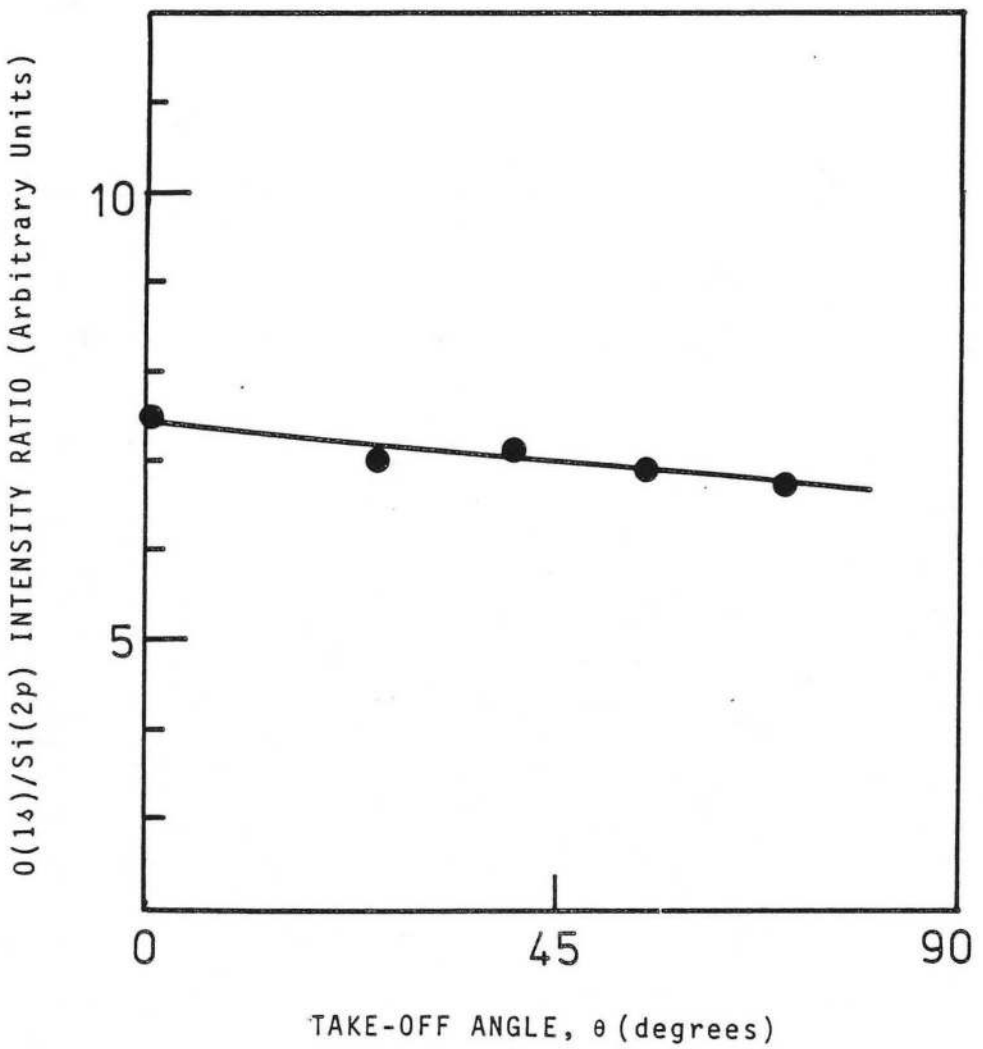

XBL 864-1660

Fig. 4

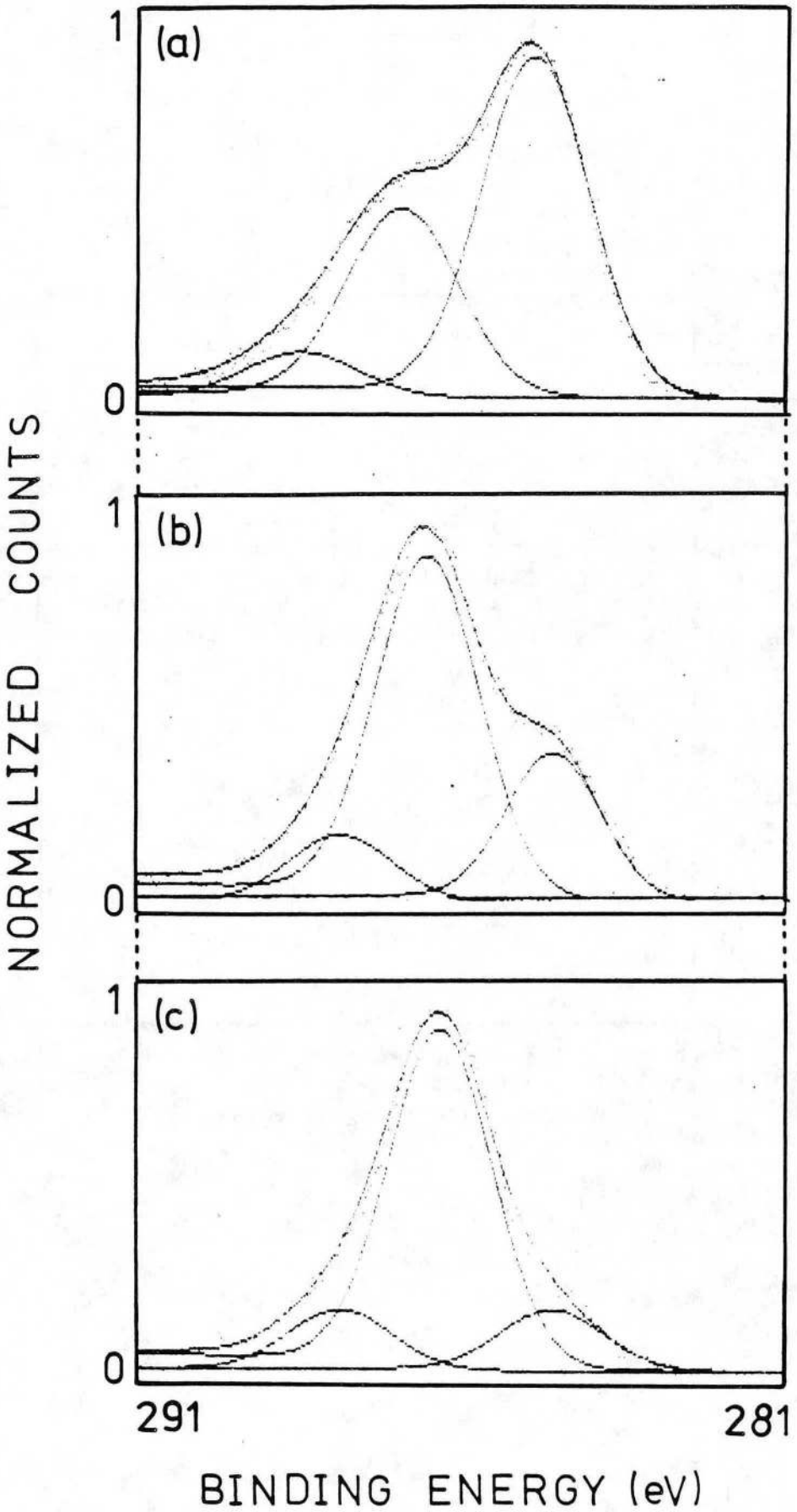

XBL 865-1726

Fig. 5

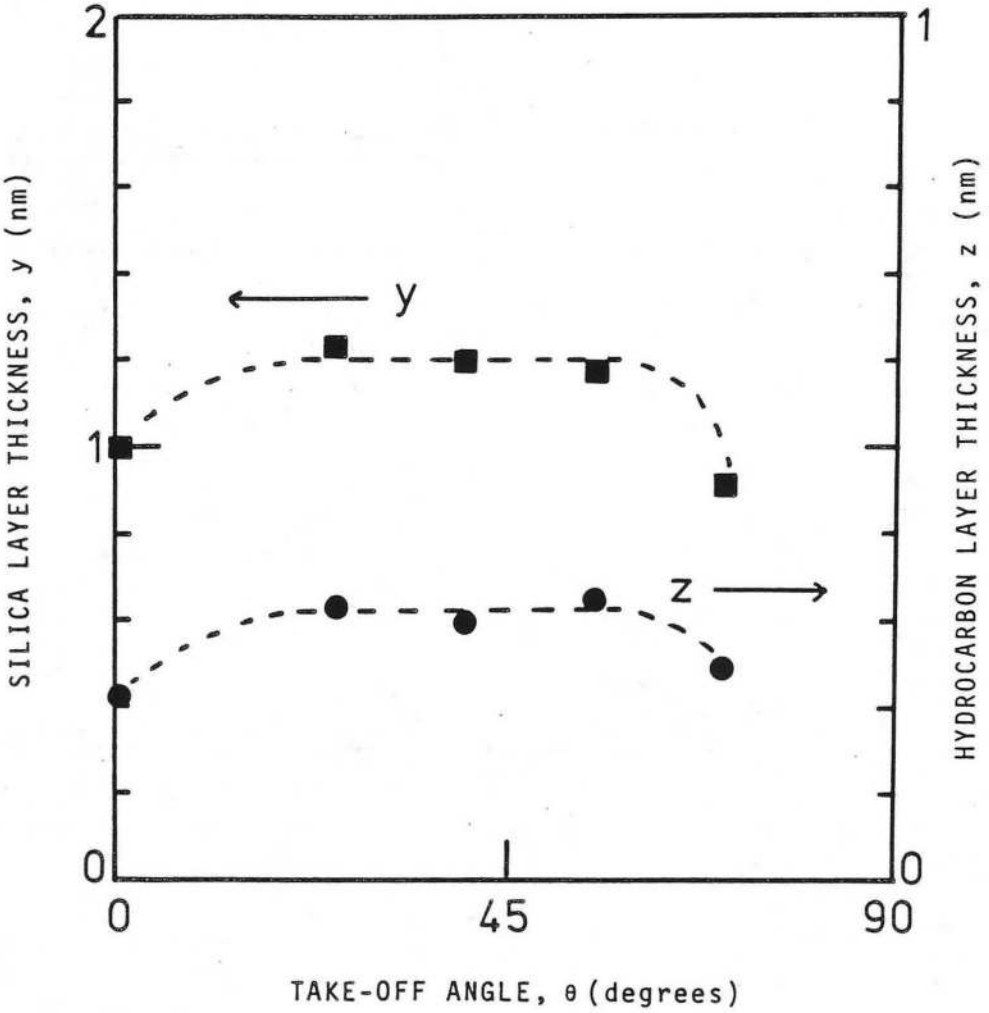

XBL 864-1661

Fig. 6

LAWRENCE BERKELEY LABORATORY
TECHNICAL INFORMATION DEPARTMENT
UNIVERSITY OF CALIFORNIA
BERKELEY, CALIFORNIA 94720